

Evidence for primordial black holes in LIGO/Virgo gravitational-wave data

Gabriele Franciolini,^{1,*} Vishal Baibhav,² Valerio De Luca,^{1,3} Ken K. Y. Ng,^{4,5}
Kaze W. K. Wong,² Emanuele Berti,² Paolo Pani,^{3,6} Antonio Riotto,¹ and Salvatore Vitale^{4,5}

¹*Département de Physique Théorique and Centre for Astroparticle Physics (CAP),
Université de Genève, 24 quai E. Ansermet, CH-1211 Geneva, Switzerland*

²*Department of Physics and Astronomy, Johns Hopkins University, 3400 N. Charles Street, Baltimore, MD 21218, USA*

³*Dipartimento di Fisica, Sapienza Università di Roma, Piazzale Aldo Moro 5, 00185, Roma, Italy*

⁴*LIGO Laboratory, Massachusetts Institute of Technology, Cambridge, Massachusetts 02139, USA*

⁵*Kavli Institute for Astrophysics and Space Research,
Massachusetts Institute of Technology, Cambridge, Massachusetts 02139, USA*

⁶*INFN, Sezione di Roma, Piazzale Aldo Moro 2, 00185, Roma, Italy,*

With approximately 50 binary black hole events detected by LIGO/Virgo to date and many more expected in the next few years, gravitational-wave astronomy is shifting from individual-event analyses to population studies aimed at understanding the formation scenarios of these sources. There is strong evidence that the black hole mergers detected so far belong to multiple formation channels. We perform a hierarchical Bayesian analysis on the GWTC-2 catalog using a combination of ab-initio astrophysical formation models (including common envelope, globular clusters, and nuclear star clusters) as well as a realistic population of primordial black holes formed in the early universe. The evidence for a primordial population is decisively favored compared to the null hypothesis and the inferred fraction of primordial black holes in the current data is estimated at $0.27^{+0.28}_{-0.24}$ (90% credible interval), a figure which is robust against different assumptions on the astrophysical populations. The primordial formation channel can explain events in the upper mass gap such as GW190521, which are in tension with astrophysical formation scenarios. Our results suggest the tantalizing possibility that LIGO/Virgo may have already detected black holes formed after inflation. This conclusion can ultimately be confirmed in the era of third-generation interferometers.

Introduction. The latest catalog of compact binary coalescence (CBC) sources published by the LIGO/Virgo collaboration (LVC) [1, 2] includes 39 CBCs, most of which are binary black holes (BBHs) [3]. This brings the total number of BBHs reported by the LVC to date to 47 [4]. Additional detections have been reported by independent groups using public data, though usually with lower statistical significance (see e.g. [5–7] and references therein). As the number of BBH observations increases, we can characterize with increasing accuracy the properties of the underlying population of black holes (BHs) and the relative contribution of various formation channels that may lead to BBH mergers.

In the analysis of BBH populations, the LVC has used phenomenological models built to capture key expected features of the mass, spin, and redshift distribution of BBHs (e.g. a power-law mass distribution), but not the physical mechanisms responsible for these features (e.g., mass transfer in binary evolution) [4]. The model that is preferred by the data describes the distribution of the primary (i.e., most massive) BH in the binary as the sum of a power-law and a Gaussian distribution, denoted as “Power Law + Peak” in Ref. [4]. The model has several free parameters and it is preferred to a simpler power-law function, which might suggest that multiple formation channels are at play. In fact, the LVC finds that $10^{+14}_{-7}\%$ of the detected BBHs belong to the Gaussian component, centered at $33.07^{+3.96}_{-5.63} M_{\odot}$.

There are many astrophysical formation scenarios that could produce the observed mergers [8, 9], and several astrophysical mechanisms could explain this excess of massive BHs. They might be the result of hierarchical mergers of smaller objects [10–14]; the end product of the life of massive stars just below the pair-instability supernova mass gap [15–17]; or of primordial origin [18, 19]. One event in particular, GW190521 [20], challenges traditional formation scenarios. With component masses of $m_1 = 90.9^{+29.1}_{-17.3} M_{\odot}$ and $m_2 = 66.3^{+19.3}_{-20.3} M_{\odot}$, GW190521 is the most massive BBH detected to date. The posterior of the primary mass has support nearly entirely in the pair-instability supernova mass gap, where BHs are not expected to form from the collapse of massive stars (see [21–26] for discussions of astrophysical uncertainties in this prediction).

In addition to astrophysical formation channels, a tantalizing possibility is that a fraction of the BBH events may be due to primordial BHs (PBHs) [27–30] formed from the collapse of large overdensities in the radiation-dominated early universe [31–34]. In this scenario, primordial BBHs are assembled via random gravitational decoupling from the Hubble flow before the matter-radiation equality [35, 36] (see [37, 38] for reviews). PBHs in different mass ranges could contribute to a sizeable fraction $f_{\text{PBH}} \equiv \Omega_{\text{PBH}}/\Omega_{\text{DM}}$ of the dark matter energy density in our universe [39], but current GW data imply an upper bound $f_{\text{PBH}} \lesssim \mathcal{O}(10^{-3})$ in the mass range of interest to current GW detectors [40–56].

Overall, the data indicate that not all BBH events detected so far can be explained by a single formation

* Gabriele.Franciolini@unige.ch

channel, be it either astrophysical [57] or primordial [52] (see [54] for the most updated analysis of the PBH scenario). Previous works tried to infer the mixing fraction of multiple astrophysical populations [57–61] and compared the PBH scenario against the phenomenological LVC power-law model [52, 55, 56]. In this Letter we report on a more extensive analysis: we perform hierarchical Bayesian inference on the GWTC-2 catalog by mixing a state-of-the-art model for the PBH population [46, 62] with several astrophysical models which can reproduce many of the features of the observed BBH mass function. This allows us to infer the evidence for PBHs in current GW data given our present knowledge of astrophysical formation scenarios.

Our astrophysical models come from the most comprehensive attempt to date at comparing different astrophysical formation scenarios against LVC data [57]. That work considered three field formation models and two dynamical formation models for BBH mergers, each with unique predictions for the evolution of merger rates with redshift, as well as the mass and spin distributions of merging binaries. Among the three field formation scenarios, Ref. [57] found that the dominant channel consists of mergers occurring through a late-phase common envelope (CE). This channel was simulated using the POSYDON framework [63], which models different phases of binary evolution with the population synthesis code COSMIC [64] and uses MESA [65] for detailed binary evolution calculations. The key parameter of the model is the CE efficiency $\alpha_{\text{CE}} \in [0.2, 0.5, 1.0, 2.0, 5.0]$: large values of α_{CE} lead to efficient CE evolution. Another key parameter is the natal BH spin $\chi_{\text{b}} \in [0, 0.1, 0.2, 0.5]$. The two models for dynamical formation in dense stellar environments consider formation in old, metal-poor globular clusters (GC) and in nuclear star clusters (NSC). The GC models are taken from a grid of 96 N -body models of collisional star clusters simulated using the cluster Monte Carlo code CMC [12]. The 96 models consist of four independent grids of 24 models, each with different initial spins. Large natal spins imply larger ejection probabilities, and therefore a smaller probability of repeated mergers. The NSC models use COSMIC to generate the BH masses from a single stellar population with metallicity $Z = (0.01, 0.1, 1)Z_{\odot}$, and evolve the clusters and their BHs using the semi-analytical approach described in [66]. This procedure is repeated for the four values of χ_{b} listed above.

For the PBH model, we compute merger rates following Refs. [46, 48, 53, 62], as in other recent studies [18, 54, 56]. The (lognormal) PBH mass function is characterized by two parameters: the central mass scale M_{c} (not to be confused with a binary’s chirp mass \mathcal{M}) and the width σ . Another hyperparameter is the abundance of PBHs, normalized with respect to the dark matter, f_{PBH} . Finally, PBHs may experience a phase of matter accretion during their cosmic evolution, impacting their mass and spin distributions at detection. The natal PBH spins are negligible as PBHs form from the collapse of radiation density perturbations in the early universe [67, 68], and therefore

the parameter χ_{b} affects only our astrophysical formation channels. To capture uncertainties in the accretion model we introduce a cut-off redshift $z_{\text{cut-off}}$ below which accretion is inefficient. If $z_{\text{cut-off}} \gtrsim 30$, accretion is negligible in the mass range of interest for LVC observations and PBHs retain small spins even at low redshift, whereas $z_{\text{cut-off}} \simeq 10$ would correspond to a strong accretion phase, leading to larger PBH masses and spins [51, 62]. Similarly to the dynamical astrophysical channels, the PBH spin orientations with respect to the binary’s angular momentum are independent and uniformly distributed on the sphere.

Overall, our astrophysical models depend on the *hyperparameters* $\lambda_{\text{ABH}} = [\alpha_{\text{CE}}, \chi_{\text{b}}, N_{\text{CE}}^{\text{det}}, N_{\text{GC}}^{\text{det}}, N_{\text{NSC}}^{\text{det}}]$, where N_i^{det} identifies the rate of detectable events of each channel during the O1/O2 and O3a runs and, following Ref. [57], is assumed to be unconstrained and independent of α_{CE} and χ_{b} . The PBH channel depends on $\lambda_{\text{PBH}} = [M_{\text{c}}, \sigma, f_{\text{PBH}}, z_{\text{cut-off}}]$, which uniquely determine the merger rate, see Eq. (3.1) of Ref. [56].

Data analysis. Our setup is the same as the one used in Refs. [54, 56]. In particular, the analysis is performed by sampling the likelihood function, defined as [69]

$$p(\lambda|\mathbf{d}) = \pi(\lambda) e^{-N_{\text{det}}(\lambda)} [N(\lambda)]^{N_{\text{obs}}} \prod_{i=1}^{N_{\text{obs}}} \frac{1}{\mathcal{S}_i} \sum_{j=1}^{\mathcal{S}_i} \frac{p_{\text{pop}}(j\theta_i|\lambda)}{\pi(j\theta_i)}, \quad (1)$$

in the space of the hyperparameters $\lambda = \lambda_{\text{ABH}} \cup \lambda_{\text{PBH}}$ by using the Markov chain Monte Carlo software algorithm *emcee* [70]. In Eq. (1), N_{obs} is the number of GW events in the catalog; $N(\lambda)$ is the number of events in the model characterized by the set of hyperparameters λ ; $N_{\text{det}}(\lambda)$ is the expected number of *observable* events in the model computed by accounting for the experimental selection bias; \mathcal{S}_i is the length of the sample taken from the posterior dataset of each event in the catalog; $\pi(\theta)$ is the prior on the binary parameters θ used by the LVC when performing the parameter estimation – this prior is removed to extract the values of the single-event likelihood, ensuring only the informative part of the event posterior is used and does not affect the population inference (but see Refs. [71–74] for its impact on the interpretation of single events); and $\pi(\lambda)$ is the prior on the hyperparameters, which is assumed to be flat.

The quantity $p_{\text{pop}}(\theta|\lambda)$ is the distribution of the BBH parameters $\theta_i = [m_1, m_2, z, \chi_{\text{eff}}]$, where m_i is the source-frame mass of the i -th binary component, z is the merger redshift, and $\chi_{\text{eff}} \equiv (\chi_1 \cos \alpha_1 + q \chi_2 \cos \alpha_2)/(1+q)$ is the effective spin parameter, which is a function of the mass ratio $q \equiv m_2/m_1 \leq 1$, of both BH spin magnitudes χ_j ($j = 1, 2$, with $0 \leq \chi_j \leq 1$), and of their orientation with respect to the orbital angular momentum, parametrized by the tilt angles α_j . In the inference we neglect the precessional spin χ_{p} , since this parameter is poorly determined for most of the GW events detected to date [4]. The Supplemental Material gives more details on the calculation of $p_{\text{pop}}(\theta|\lambda)$.

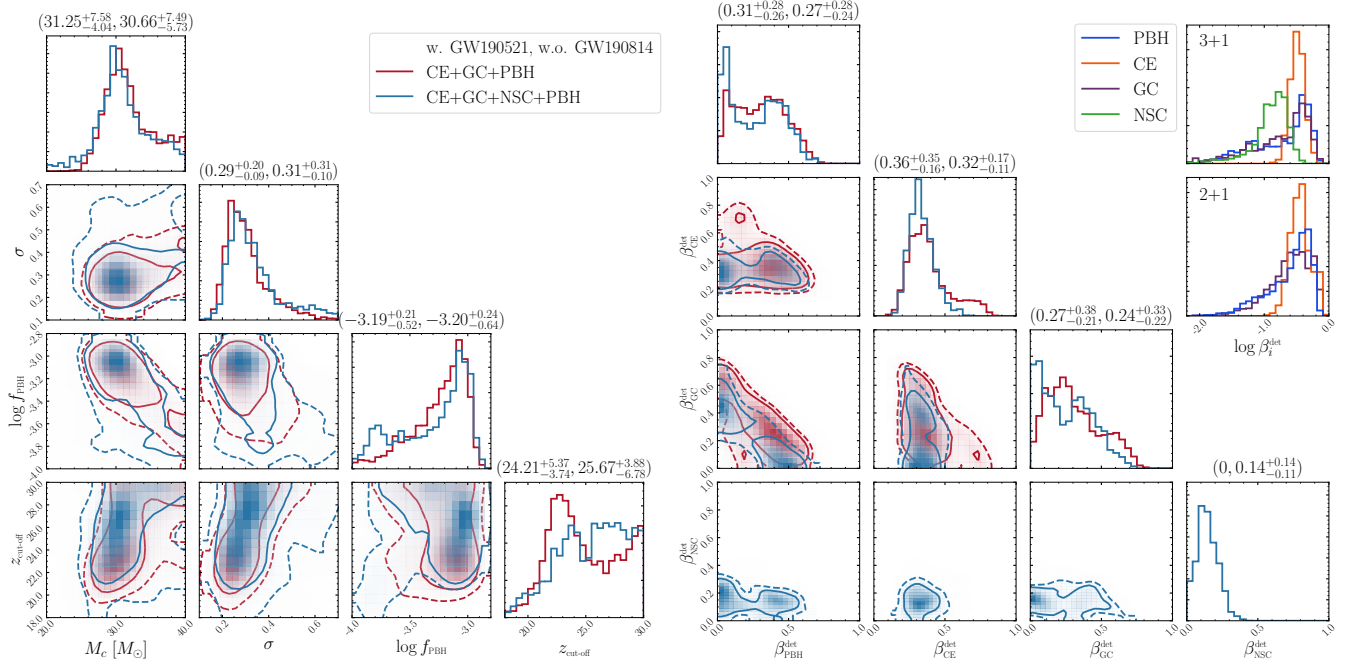


FIG. 1: Posterior distributions of the hyperparameters of the PBH model (left panel) and of the individual *detectable* mixing fractions β_i^{det} of different populations (right panel) for the CE+GC+PBH model (red, 2+1) and for the CE+GC+NSC+PBH mixed model (blue, 3+1). We include GW190521 in the catalog, but not GW190814. The 90% credible interval reported at the top of each column corresponds to the CE+GC+PBH (left) and CE+GC+NSC+PBH (right) mixed models, respectively. The inset in the top right corner shows the individual β_i^{det} in logarithmic scale to highlight the monotonic behaviour at small fractions.

To quantify the statistical evidence of various models given the GWTC-2 dataset, one can compute the Bayes factor between model \mathcal{M}_1 and model \mathcal{M}_2 , namely $\mathcal{B}_{\mathcal{M}_2}^{\mathcal{M}_1} \equiv Z_{\mathcal{M}_1}/Z_{\mathcal{M}_2}$, where $Z_{\mathcal{M}} \equiv \int d\lambda p(\lambda|\mathbf{d})$ is the evidence. According to Jeffreys' scale criterion [75], a Bayes factor larger than $(10, 10^{1.5}, 10^2)$ would imply a strong, very strong, or decisive evidence in favor of model \mathcal{M}_1 with respect to model \mathcal{M}_2 given the available data.

Results. Among all the CBC events included in the GWTC-2 catalog, we discard three events with large false-alarm rate (GW190426, GW190719, GW190909) [4] and two events involving neutron stars (GW170817, GW190425). GW190814 [76] requires a separate treatment, since its secondary mass ($m_2 \approx 2.6 M_\odot$) would correspond to either the lowest-mass astrophysical BH or to the highest-mass neutron star observed to date, challenging our current understanding of compact objects. For the moment we assume that the secondary component of GW190814 is a neutron star and neglect this event.

Unlike Ref. [57], we include GW190521 [20] in the catalog. At least the primary component of GW190521 lies in the (upper) mass gap predicted by the pair-instability supernova theory, in tension with most astrophysical models (see [21–26]), while being compatible with the PBH scenario [18]. Overall, the selected catalog contains $N_{\text{obs}} = 44$ events.

The results of our hierarchical Bayesian analysis

are summarized in Fig. 1, which shows the posterior distributions of the hyperparameters of the PBH model (left panel) and of the detectable mixing fractions $\beta_i^{\text{det}} = N_i^{\text{det}} / \sum_j N_j^{\text{det}}$ (right panel), where $i, j = \{\text{CE}, \text{GC}, \text{NSC}, \text{PBH}\}$ for the different models. We present both the most conservative scenario in which the PBH population is mixed with all three astrophysical models (CE, GC, NSC) and the case in which the NSC subpopulation is excluded.

The posterior distributions in these two cases are overall similar. In the CE+GC+PBH mixed model, the distribution of $z_{\text{cut-off}}$ shows two peaks at $z_{\text{cut-off}} \approx 23$ and $z_{\text{cut-off}} \approx 30$. The first corresponds to the case where some PBH accretion is necessary to explain the (few) spinning events in the catalog [51, 62], while the second peak corresponds to the case when the observed events associated to PBHs by the inference are mostly nonspinning. In the CE+GC+NSC+PBH mixed case, the posterior of $z_{\text{cut-off}}$ is approximately flat above $z_{\text{cut-off}} \sim 25$, which is possibly explained by the fact that fewer events with nonnegligible spin are assigned to PBHs. We have also checked that the posterior remains flat for $z_{\text{cut-off}} \gtrsim 30$, where accretion is indeed negligible in the mass range of interest.

In Table I, we present the Bayes factors for the different combinations of mixed populations with and without a PBH subpopulation. First of all, we notice that the Bayes factors do not favor the scenarios incorporating

TABLE I: Bayesian evidence ratios for the different combinations of mixed populations with and without a PBH subpopulation, obtained by marginalising over α_{CE} and χ_b and including GW190521.

Model \mathcal{M}	CE+GC	CE+GC+NSC	CE+GC+PBH	CE+GC+NSC+PBH
$\log_{10} \mathcal{B}_{\text{CE+GC}}^{\mathcal{M}}$	0	-0.15	2.38	2.30

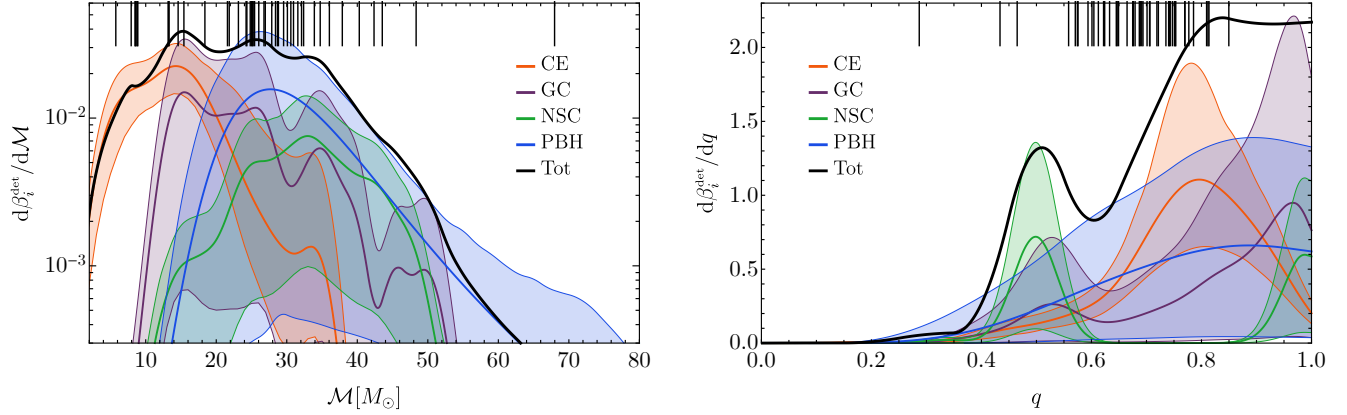


FIG. 2: Individual contribution to the observable distributions of chirp mass (left) and mass ratio (right) for each population model in the CE+GC+NSC+PBH scenario. The analogous plots for the CE+GC+PBH scenario are shown in the Supplemental Material. The bands indicate 90% credible intervals, while the black line corresponds to the mean total population. Vertical lines at the top of each plot correspond to the mean observed values for the events in the GWTC-2 catalog.

the NSC channel. This is because, even though NSC helps in accounting for events in the central range of chirp masses in the catalog, GW190521 still remains an outlier of the combined population, thus the inclusion of the additional dynamical channel does not lead to a larger evidence. The PBH channel is able to efficiently produce binaries in the mass gap (explaining GW190521) and therefore the corresponding Bayes factor is larger, $\log_{10} \mathcal{B}_{\text{no PBH}}^{\text{PBH}} \simeq 2.3$, showing a decisive evidence for a mixed astrophysical+primordial model. Its inclusion also helps in accounting for some of the heavy events other than GW190521. This is reflected into a significant PBH fraction $\beta_{\text{PBH}}^{\text{det}} = 0.31^{+0.28}_{-0.26}$ ($0.27^{+0.28}_{-0.24}$) at 90% C.L. in the CE+GC+PBH (CE+GC+NSC+PBH) mixed scenario, as shown in Fig. 1. The inclusion of the NSC channel does not improve the overall fit, since this channel is mostly competitive with the GC one, whereas an anti-correlation exists between the PBH and GC posteriors. As shown in the inset of Fig. 1, the posterior of the PBH mixing fraction does not have support at $\beta_{\text{PBH}}^{\text{det}} \approx 0$, since at least GW190521 can only be ascribed to the PBH channel. Indeed, the first percentile of $\beta_{\text{PBH}}^{\text{det}}$ is 0.022 (0.014) for the CE+GC+PBH (CE+GC+NSC+PBH) mixed scenario.

Nonetheless, as shown in more detail in the Supplemental Material, the fraction of PBHs in the catalog does not depend significantly on the inclusion of GW190521 and/or GW190814, and on the number of astrophysical models contributing to the entire population. In particular, al-

though GW190521 challenges the standard astrophysical formation scenarios, there is evidence for PBHs in the catalog even without including this event in the analysis. In all cases, $\beta_{\text{PBH}}^{\text{det}} = 0$ is outside the 90% confidence interval.

Finally, in order to qualitatively understand how the GWTC-2 events are interpreted by the inference, in Fig. 2 we plot the contribution of each population model to the distributions of the chirp mass (left) and mass ratio (right). The chirp mass distributions show that the PBH population overlaps mostly with the GC channel (and with NSC, when included in the inference) but extends to larger values of \mathcal{M} . The necessity for the PBH distribution to reach the mass gap event makes it less competitive in explaining the bulk of events in the central range of chirp masses. This is the reason why the posterior of $\log_{10} f_{\text{PBH}}$ has a significant tail at small values, corresponding to the subdominant peak in the mixing fraction $\beta_{\text{PBH}}^{\text{det}}$ (see Fig. 1). This does not happen when GW190521 is removed, since then the PBH model can efficiently produce the bulk of events in the central range of \mathcal{M} . Finally, note that the CE channel consistently explains the light events in the catalog in all cases.

Discussion. A mixed population of BBHs from different astrophysical channels can in principle reproduce many features of the current BBH catalog, except possibly for the upper-mass-gap event GW190521 [57]. Thus, it is quite remarkable that – after adding a further population of PBHs – the inferred PBH mixing fraction is significant.

Our Bayesian analysis shows that not only does a PBH population naturally explain very massive binaries such as GW190521, but the overall PBH fraction robustly lies at $27^{+28}_{-24}\%$ of the total number of detections, being statistically favored against competitive astrophysical population models such as GC and NSC.

If confirmed, these results would imply that the LVC could have already detected up to 24 BBHs formed in the early universe. Given the potential impact of such a discovery, it is necessary to corroborate our analysis. We adopted a standard lognormal distribution for the PBH mass function at formation, but it would be important to test the impact of different choices. Likewise, we have considered three state-of-the-art astrophysical models [57], but there might exist others (especially belonging to the dynamical formation scenario) which are competitive against the primordial subpopulation.

Confidently confirming the primordial nature of some BBHs would probably require individual-event analyses for large signal-to-noise ratio events, especially by cross-correlating merger rates with mass, spin, and redshift measurements to identify key features of the PBH scenario (see e.g. [74] for work in this direction). Another possibility to break the degeneracy between the PBH and astrophysical channels is to perform population studies focusing on spin distributions [77, 78], and accounting for the $q - \chi_{\text{eff}}$ correlation introduced by accretion effects in PBH models [51, 62].

Ultimately, a confirmation of the primordial nature of a subpopulation of BBHs will come from third-generation GW detectors, such as the Einstein Telescope [79] and Cosmic Explorer [80], which will detect BH mergers up to $z \approx 50$ [81], and can in principle reconstruct the redshift evolution of the merger rate (although the accuracy of the redshift measurement deteriorates with redshift [82, 83]). The merger rate is monotonically increasing with redshift for primordial BBHs, whereas it should peak around redshift of a few for astrophysical BBHs, and at $z \approx (10 - 20)$ for BHs formed from the first stars [84–86], (see [83, 87–91] for recent studies). In this context, it is interesting to note that our results for the PBH fraction in current data are in agreement with the simplified analysis performed in [56] using the LVC power-law model for the astrophysical population. In particular, by mapping the currently inferred fraction of PBHs to the merger rates for third-generation detectors, one would expect to detect dozens to hundreds BBH events at $z \gtrsim 30$, which might therefore be identified as being primordial [56, 92], provided an accurate measurement of the redshift for these very distant events will be achievable [83]. Alternatively, another test of the presence of PBH events in GW data may come from a dedicated population analysis of the events measurable at high redshifts by third-generation interferometers, thus exploiting statistical tools to increase the information on the merger rate evolution [93].

Acknowledgments. We are very grateful to M. Zevin for insightful discussions about Ref. [57] and help in using the publicly available repository [94]. Some computa-

tions were performed at the University of Geneva on the Baobab/Yggdrasil cluster and at Sapienza University of Rome on the Vera cluster of the Amaldi Research Center funded by the MIUR program “Dipartimento di Eccellenza” (CUP: B81I18001170001). E. Berti, V. Baibhav and K. W. K. Wong are supported by NSF Grants No. PHY-1912550 and AST-2006538, NASA ATP Grants No. 17-ATP17-0225 and 19-ATP19-0051, NSF-XSEDE Grant No. PHY-090003, and NSF Grant PHY-20043. This work has received funding from the European Union’s Horizon 2020 research and innovation programme under the Marie Skłodowska-Curie grant agreement No. 690904. This research project was conducted using computational resources at the Maryland Advanced Research Computing Center (MARCC). V.D.L., G.F. and A.R. are supported by the Swiss National Science Foundation (SNSF), project *The Non-Gaussian Universe and Cosmological Symmetries*, project number: 200020-178787. P.P. acknowledges financial support provided under the European Union’s H2020 ERC, Starting Grant agreement no. DarkGRA-757480, under the MIUR PRIN and FARE programmes (GW-NEXT, CUP: B84I20000100001). K. K. Y. N. and S. V., members of the LIGO Laboratory, acknowledge the support of the National Science Foundation through the NSF Grant No. PHY-1836814. LIGO was constructed by the California Institute of Technology and Massachusetts Institute of Technology with funding from the National Science Foundation and operates under Cooperative Agreement No. PHY-1764464. The authors would like to acknowledge networking support by the GWverse COST Action CA16104, “Black holes, gravitational waves and fundamental physics.”

This research has made use of data, software and/or web tools obtained from the Gravitational Wave Open Science Center (<https://www.gw-openscience.org/>), a service of LIGO Laboratory, the LIGO Scientific Collaboration and the Virgo Collaboration. LIGO Laboratory and Advanced LIGO are funded by the United States National Science Foundation (NSF) as well as the Science and Technology Facilities Council (STFC) of the United Kingdom, the Max-Planck-Society (MPS), and the State of Niedersachsen/Germany for support of the construction of Advanced LIGO and construction and operation of the GEO600 detector. Additional support for Advanced LIGO was provided by the Australian Research Council. Virgo is funded, through the European Gravitational Observatory (EGO), by the French Centre National de Recherche Scientifique (CNRS), the Italian Istituto Nazionale di Fisica Nucleare (INFN) and the Dutch Nikhef, with contributions by institutions from Belgium, Germany, Greece, Hungary, Ireland, Japan, Monaco, Poland, Portugal, Spain.

Appendix A: Supplemental Material

Here we provide details on our data analysis and further results complementary to those presented in the main text.

TABLE II: Prior ranges for the hyperparameters of the primordial and astrophysical models. We assume uniform distributions for all parameters. Following Ref. [57], we considered discrete values for the hyperparameters α_{CE} and χ_{b} . Binary components spinning at $\chi < \chi_{\text{b}}$ at BBH formation are given spins of χ_{b} . We recall that α_{CE} only affects the CE model.

Model	PBH				ABH	
Parameter	$M_c [M_\odot]$	σ	$\log f_{\text{PBH}}$	$z_{\text{cut-off}}$	α_{CE}	χ_{b}
Prior range	[10, 40]	[0.1, 1.1]	[-4, -2]	[10, 30]	[0.2, 0.5, 1, 2, 5]	[0, 0.1, 0.2, 0.5]

1. Details of the data analysis

The key quantity to be evaluated is the likelihood function $p(\boldsymbol{\lambda}|\mathbf{d})$, defined in Eq. (1) of the main text. Here we explain how its various ingredients are computed.

The priors on the hyperparameters $\pi(\boldsymbol{\lambda})$ are uniformly distributed in the ranges given in Table II. Note that at values of the cut-off redshift above $z_{\text{cut-off}} \gtrsim 30$, and in the mass range of interest, accretion onto PBHs is negligible [62]. Therefore, all models with $z_{\text{cut-off}} \gtrsim 30$ are degenerate and we can cut the range at this reference value, as done in Refs. [54, 56].

The binary parameter distributions in a given model (either primordial or astrophysical) can be computed from the differential merger rate $dR/(dm_1 dm_2)$ as

$$p_{\text{pop}}(\boldsymbol{\theta}|\boldsymbol{\lambda}) \equiv \frac{1}{N(\boldsymbol{\lambda})} \left[T_{\text{obs}} \frac{1}{1+z} \frac{dV}{dz} \frac{dR}{dm_1 dm_2}(\boldsymbol{\theta}|\boldsymbol{\lambda}) \right], \quad (\text{A1})$$

with T_{obs} being the observation time, whereas the number of expected detections reads

$$N_{\text{det}}(\boldsymbol{\lambda}) \equiv T_{\text{obs}} \int dm_1 dm_2 dz p_{\text{det}}(m_1, m_2, z) \times \frac{1}{1+z} \frac{dV}{dz} \frac{dR}{dm_1 dm_2}(m_1, m_2, z|\boldsymbol{\lambda}), \quad (\text{A2})$$

where the prefactor $1/(1+z)$ accounts for the redshift at the source epoch and dV/dz stands for the differential comoving volume factor, see e.g. [95]. We account for selection bias by introducing the probability of detection

$$p_{\text{det}}(\theta_i) = \int p(\theta_e) \Theta[\rho(\theta_i, \theta_e) - \rho_{\text{thr}}] d\theta_e, \quad (\text{A3})$$

where $\theta_i = \{m_1, m_2, z\}$ are the intrinsic parameters of the binary (individual source-frame masses m_i and merger redshift z), whereas $\theta_e = \{\alpha, \delta, \iota, \psi\}$ are the extrinsic parameters (right ascension α , declination δ , orbital-plane inclination ι , and polarization angle ψ). Finally, $p(\theta_e)$ is the probability distribution function of θ_e , Θ is the Heaviside step function, and ρ is the signal-to-noise ratio (SNR). For simplicity we neglect the spins χ_i ($i = 1, 2$) in the computation of the detectability, since the large majority of the GWTC-2 events are compatible with zero spin.

In the case of the GWTC-1 catalog, p_{det} can be computed in the approximate single-detector semianalytic framework of Refs. [96, 97] and adopting a SNR threshold

$\rho_{\text{thr}} = 8$ without encountering significant departures from the large-scale injection campaigns in the O1 [98] and O2 [99] runs. We adopt the same procedure to compute the detectability of binaries also for the O3a run.

The SNR can be factored out as $\rho(\theta_i, \theta_e) = \omega(\theta_e) \rho_{\text{opt}}(\theta_i)$, where ρ_{opt} is the SNR of an “optimal” source located overhead the detector with face-on inclination. The optimal SNR ρ_{opt} of individual GW events is given in terms of the (Fourier-transformed) GW waveform by

$$\rho_{\text{opt}}^2(m_1, m_2, \chi_1, \chi_2, z) \equiv \int_0^\infty \frac{4|\tilde{h}(\nu)|^2}{S_n(\nu)} d\nu, \quad (\text{A4})$$

where S_n is the strain noise of the detector. Following the choice adopted in Ref. [57], we adopt the `midhighlatelow` noise power spectral densities [100], as implemented in the publicly available repository `pycbc` [101].

Finally, we explicitly compute the marginalized distribution $p_{\text{det}}(\theta_i)$ [Eq. (A3)] by evaluating the cumulative distribution function $P(\omega_{\text{thr}}) = \int_{\omega_{\text{thr}}}^1 p(\omega') d\omega'$ at $\omega_{\text{thr}} = \rho_{\text{thr}}/\rho_{\text{opt}}(\theta_i)$. We consider isotropic sources, so that $\alpha, \cos \delta, \cos \iota$, and ψ are uniformly distributed. Then, for the case of a single-detector approximation, nonprecessing binaries, and considering only the dominant quadrupolar mode, the function $P(\omega_{\text{thr}})$ is found as in Ref. [95].

As discussed in the main text, we use the GWTC-2 catalog [4], discarding three events with large false-alarm rate (GW190426, GW190719, GW190909) and two events involving neutron stars (GW170817, GW190425). The cases of GW190814 [76] and GW190521 [20] require special treatment. The former can be a BH-neutron-star binary with a very massive neutron star, whereas the latter is in tension with the main astrophysical formation channels, since its primary lies within the pair-instability mass gap predicted by supernova theory. In the following, in order to remain agnostic about the nature of GW190814, we shall present the results of our analysis both with and without this event, showing that its inclusion does not alter our results. Furthermore, in order to make a more direct comparison to population models of astrophysical origin only, we shall present the results of our analysis with and without GW190521. Overall, the selected catalog contains 43 events + GW190521 + GW190814, hence $N_{\text{obs}} = 43, 44, 45$, depending on the setup. Similarly to Ref. [57], we adopt the “Combined” samples for the GWTC-1 events as provided in [102], and the “PublicationSamples” in [103] for the GWTC-2 events.

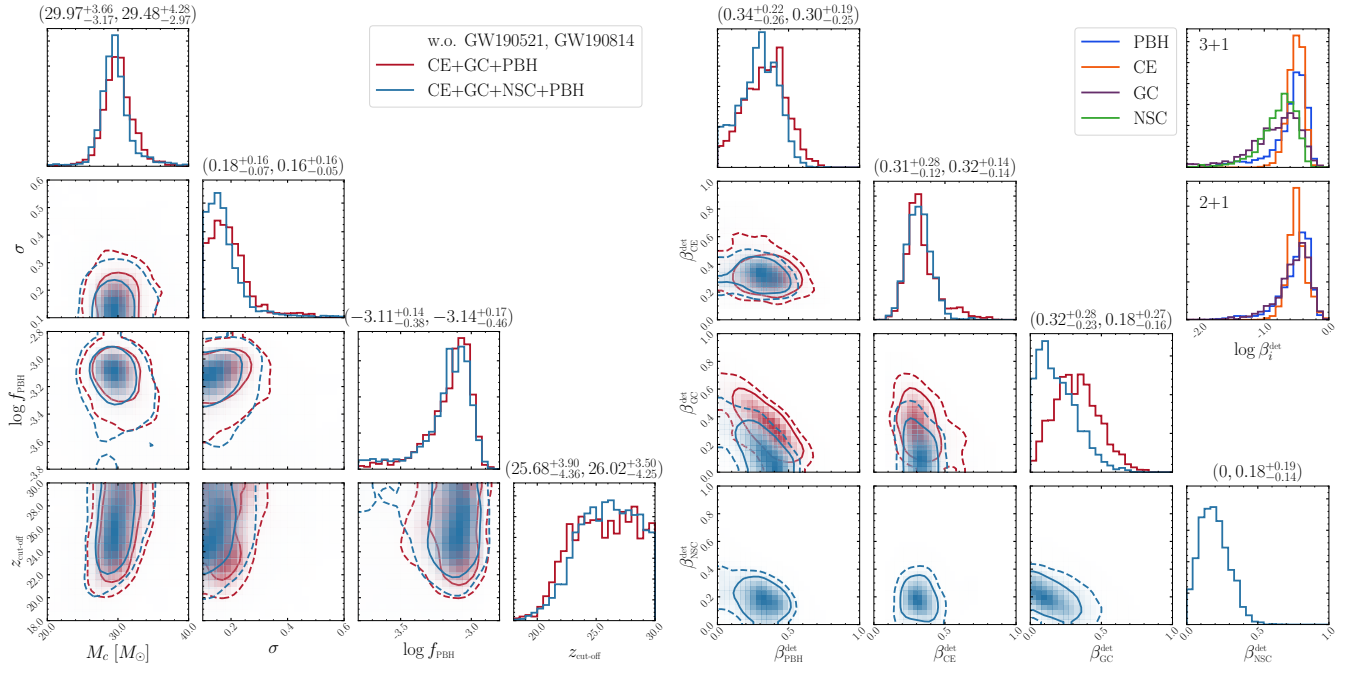


FIG. 3: Same as Fig. 1 in the main text but discarding both GW190521 and GW190814 events.

TABLE III: Bayesian evidence ratios for the different combinations of mixed populations with and without a PBH subpopulation, obtained by marginalising over α_{CE} and χ_b and excluding GW190521, since the latter event does not fit in any astrophysical model. This table can be compared to Table I in the main text, in which GW190521 was included, increasing the overall evidence for a PBH subpopulation.

Model \mathcal{M}	CE+GC	CE+GC+NSC	CE+GC+PBH	CE+GC+NSC+PBH
$\log_{10} \mathcal{B}_{\text{CE+GC}}^{\mathcal{M}}$	0	0.52	1.22	1.43

2. Supplemental results

In Fig. 3, we show the same posterior distributions as in Fig. 1 of the main text, but discarding GW190521. We consider both the CE+GC+PBH mixed population (red) and the CE+GC+NSC+PBH model (blue). The inclusion of the NSC subpopulation does not affect the posteriors significantly, except for reducing the fraction of BBHs from GCs (and to a less extent that of PBHs) in favor of a non-negligible fraction of BBHs from NSCs. By comparing the blue and red distributions, we see that a striking feature of Fig. 3 is the similarity of the inferred PBH population when different combinations of the astrophysical models are considered. Also, the posterior distribution describing the observable fractions β_i^{det} show that the CE channel is mostly uncorrelated with both the remaining astrophysical and primordial channels. On the other hand, the fraction of GC binaries is strongly anti-correlated with the PBH one and, to a lesser extent, to $\beta_{\text{NSC}}^{\text{det}}$ when this subpopulation is included. This degeneracy produces a widening of the individual 90% C.L. intervals for the GC, NSC and PBH channels.

Likewise, since GW190521 is in tension with the CE,

GC, and NSC scenarios, in Table III we present the Bayes factors for different combinations of mixed models in the case in which GW190521 is excluded from the catalog. At odds with the case discussed in the main text, the inclusion of the NSC channel is weakly preferred, in agreement with [57]. In general the models including the PBH channel are strongly preferred, with $\log_{10} \mathcal{B}_{\text{no PBH}}^{\text{PBH}} \simeq 1$, both with and without the inclusion of NSC. The Bayes factors supporting the scenarios with PBHs are smaller compared to the case with GW190521 discussed in the main text, as the mass gap event, playing an important role in determining the evidence in favor of PBHs, is absent in this case. On the other hand, the posterior distribution of $\beta_{\text{PBH}}^{\text{det}}$ has a smaller support at low fractions, as the reconstructed PBH population is able to explain more efficiently many events in the central range of chirp masses (see Figs. 4b and 4c) with respect to the case with GW190521 discussed in the main text (shown in Figs. 2 and 4a). This is also confirmed by the larger first percentile of $\beta_{\text{PBH}}^{\text{det}}$, which we find to be 0.030 (0.022) for the CE+GC+PBH (CE+GC+NSC+PBH) mixed scenario.

We also checked the robustness of our results against the inclusion of the asymmetric merger GW190814. In

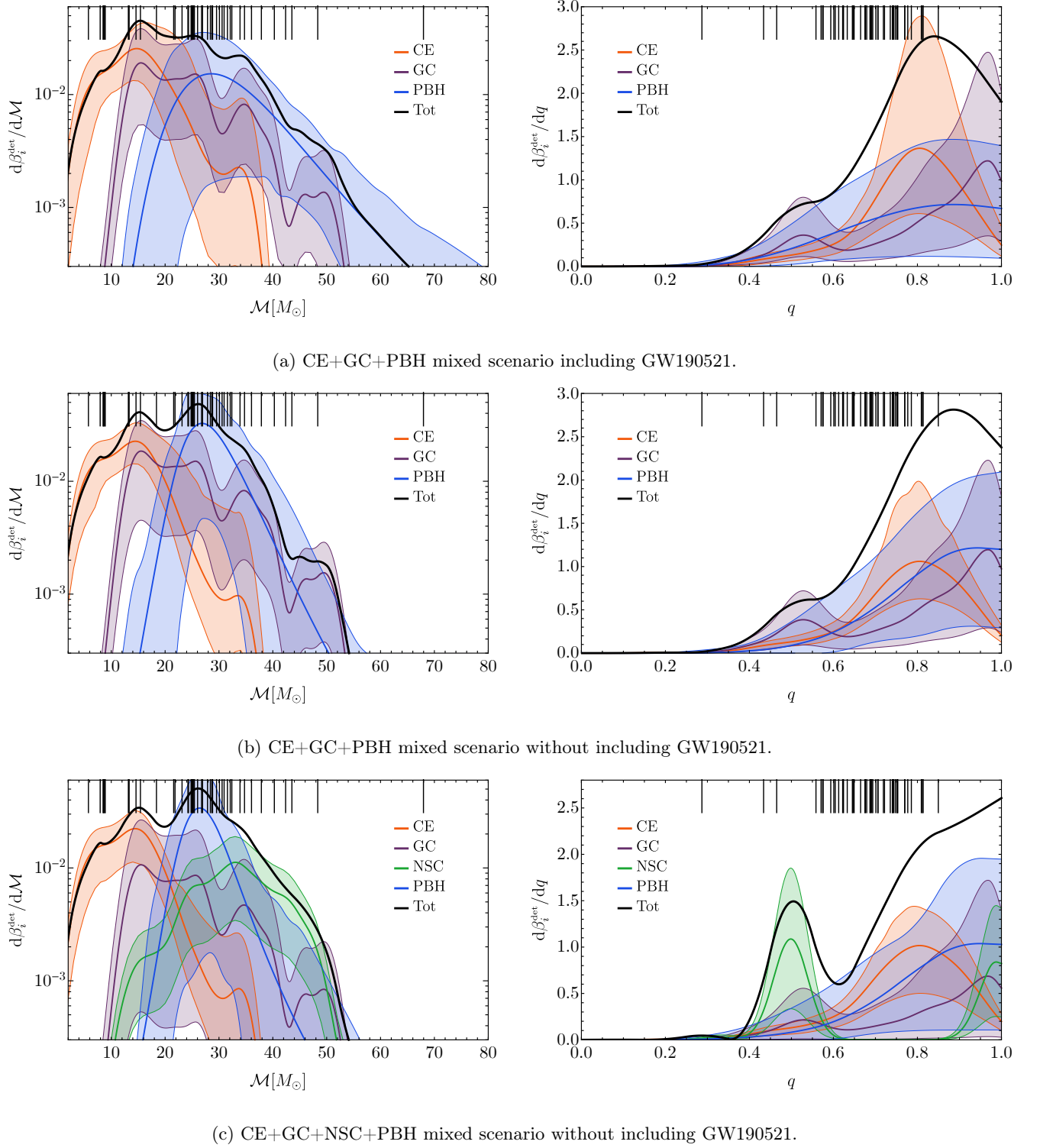


FIG. 4: Individual contribution to the observable distributions of chirp mass (left) and mass ratio (right) for each population model considered. The bands indicate 90% credible intervals, while the black line corresponds to the mean total population. Vertical lines at the top of each plot correspond to the mean observed values for the events in the GWTC-2 catalog. The CE+GC+NSC+PBH scenario including GW190521 is shown in the main text.

Fig. 5, we compare the posterior distributions obtained including/excluding GW190521 and GW190814 in var-

ious combinations for the CE+GC+PBH mixed model. Besides a modification of the posterior of the width σ of

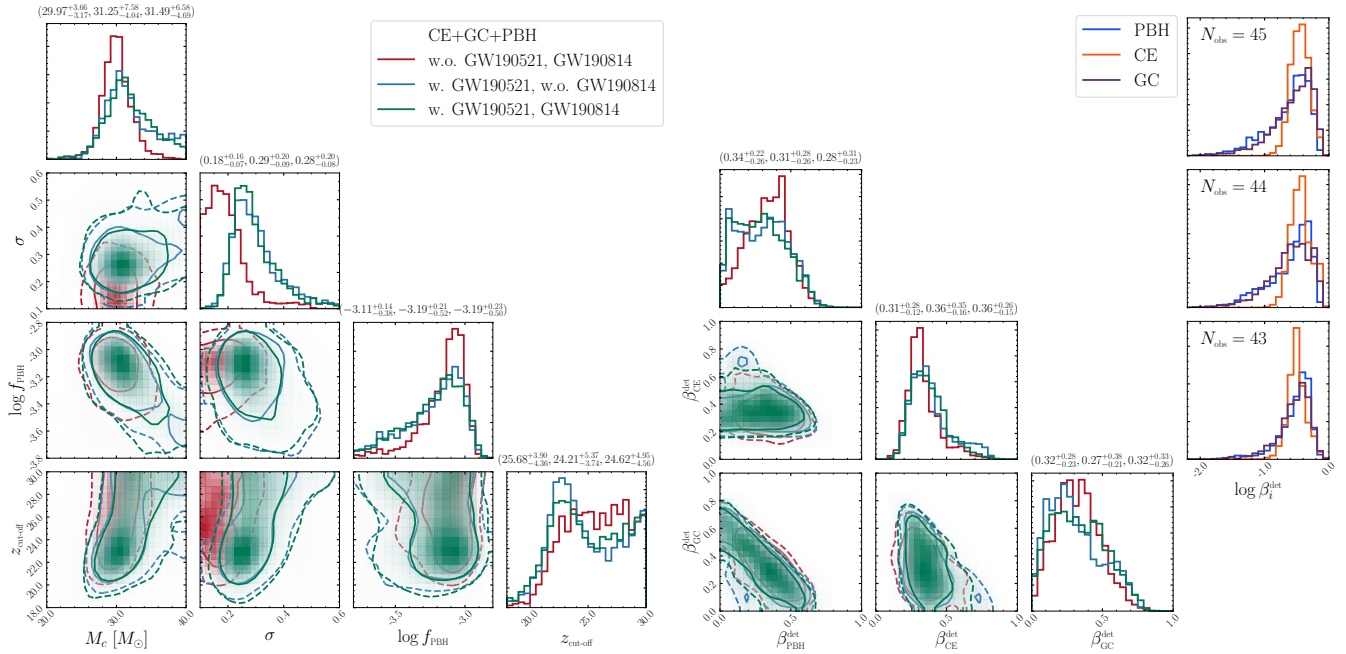


FIG. 5: Same as Fig. 1 in the main text for the CE+GC+PBH mixed model. Each color corresponds to the case both GW190521 and GW190814 are neglected (red, $N_{\text{obs}} = 43$), only GW190521 is additionally included (blue, $N_{\text{obs}} = 44$) and both GW190521 and GW190814 are included (green, $N_{\text{obs}} = 45$). The 90% C.I. reported on top of each column correspond to the various cases, following (red, blue, green) ordering.

the lognormal PBH mass function at formation (which becomes narrower and peaks at smaller values when both GW190521 and GW190814 are excluded), the other distributions are all very similar to each other, showing that the inclusion/exclusion of these two single events in the large catalog does not significantly affect the analysis, as

expected. The inclusion of GW190814 has a mild effect: this event is ascribed to the CE population, since the latter has the strongest support at small masses. The inclusion of GW190521 increases the PBH fraction at the expenses of the GC model, which is competitive at high masses.

-
- [1] J. Aasi *et al.* (LIGO Scientific), *Class. Quant. Grav.* **32**, 074001 (2015), [arXiv:1411.4547 \[gr-qc\]](#).
 - [2] F. Acernese *et al.* (VIRGO), *Class. Quant. Grav.* **32**, 024001 (2015), [arXiv:1408.3978 \[gr-qc\]](#).
 - [3] R. Abbott *et al.* (LIGO Scientific, Virgo), (2020), [arXiv:2010.14527 \[gr-qc\]](#).
 - [4] R. Abbott *et al.* (LIGO Scientific, Virgo), (2020), [arXiv:2010.14533 \[astro-ph.HE\]](#).
 - [5] A. H. Nitz, T. Dent, G. S. Davies, S. Kumar, C. D. Capano, I. Harry, S. Mozzon, L. Nuttall, A. Lundgren, and M. Tápai, *Astrophys. J.* **891**, 123 (2020), [arXiv:1910.05331 \[astro-ph.HE\]](#).
 - [6] B. Zackay, L. Dai, T. Venumadhav, J. Roulet, and M. Zaldarriaga, (2019), [arXiv:1910.09528 \[astro-ph.HE\]](#).
 - [7] J. Roulet, T. Venumadhav, B. Zackay, L. Dai, and M. Zaldarriaga, *Phys. Rev. D* **102**, 123022 (2020), [arXiv:2008.07014 \[astro-ph.HE\]](#).
 - [8] I. Mandel and A. Farmer, (2018), [arXiv:1806.05820 \[astro-ph.HE\]](#).
 - [9] M. Mapelli, *Proceedings, 200th Course of Enrico Fermi School of Physics: Gravitational Waves and Cosmology (GW-COSM): Varenna (Lake Como) (Lecco), Italy*, *Proc. Int. Sch. Phys. Fermi* **200**, 87 (2020), [arXiv:1809.09130 \[astro-ph.HE\]](#).
 - [10] D. Gerosa and E. Berti, *Phys. Rev. D* **95**, 124046 (2017), [arXiv:1703.06223 \[gr-qc\]](#).
 - [11] M. Fishbach, D. E. Holz, and B. Farr, *Astrophys. J. Lett.* **840**, L24 (2017), [arXiv:1703.06869 \[astro-ph.HE\]](#).
 - [12] C. L. Rodriguez, M. Zevin, P. Amaro-Seoane, S. Chatterjee, K. Kremer, F. A. Rasio, and C. S. Ye, *Phys. Rev. D* **100**, 043027 (2019), [arXiv:1906.10260 \[astro-ph.HE\]](#).
 - [13] D. Gerosa and E. Berti, *Phys. Rev. D* **100**, 041301 (2019), [arXiv:1906.05295 \[astro-ph.HE\]](#).
 - [14] D. Gerosa, N. Giacobbo, and A. Vecchio, (2021), [arXiv:2104.11247 \[astro-ph.HE\]](#).
 - [15] A. Heger and S. E. Woosley, *Astrophys. J.* **567**, 532 (2002), [arXiv:astro-ph/0107037 \[astro-ph\]](#).
 - [16] K. Belczynski *et al.*, *Astron. Astrophys.* **594**, A97 (2016), [arXiv:1607.03116 \[astro-ph.HE\]](#).
 - [17] V. Gayathri, Y. Yang, H. Tagawa, Z. Haiman, and I. Bartos, (2021), [arXiv:2104.10253 \[gr-qc\]](#).
 - [18] V. De Luca, V. Desjacques, G. Franciolini, P. Pani,

- and A. Riotto, *Phys. Rev. Lett.* **126**, 051101 (2021), [arXiv:2009.01728 \[astro-ph.CO\]](#).
- [19] K. Kritos, V. De Luca, G. Franciolini, A. Kehagias, and A. Riotto, (2020), [arXiv:2012.03585 \[gr-qc\]](#).
- [20] R. Abbott *et al.* (LIGO Scientific, Virgo), *Phys. Rev. Lett.* **125**, 101102 (2020), [arXiv:2009.01075 \[gr-qc\]](#).
- [21] R. Farmer, M. Renzo, S. E. de Mink, P. Marchant, and S. Justham, (2019), 10.3847/1538-4357/ab518b, [arXiv:1910.12874 \[astro-ph.SR\]](#).
- [22] J. Sakstein, D. Croon, S. D. McDermott, M. C. Straight, and E. J. Baxter, *Phys. Rev. Lett.* **125**, 261105 (2020), [arXiv:2009.01213 \[gr-qc\]](#).
- [23] K. Belczynski, *Astrophys. J. Lett.* **905**, L15 (2020), [arXiv:2009.13526 \[astro-ph.HE\]](#).
- [24] G. Costa, A. Bressan, M. Mapelli, P. Marigo, G. Iorio, and M. Spera, *Mon. Not. Roy. Astron. Soc.* **501**, 4514 (2021), [arXiv:2010.02242 \[astro-ph.SR\]](#).
- [25] S. E. Woosley and A. Heger, (2021), [arXiv:2103.07933 \[astro-ph.SR\]](#).
- [26] E. J. Baxter, D. Croon, S. D. McDermott, and J. Sakstein, (2021), [arXiv:2104.02685 \[astro-ph.CO\]](#).
- [27] Y. B. Zel'dovich and I. D. Novikov, *Soviet Astron. AJ (Engl. Transl.)*, **10**, 602 (1967).
- [28] S. W. Hawking, *Nature* **248**, 30 (1974).
- [29] G. F. Chapline, *Nature* **253**, 251 (1975).
- [30] B. J. Carr, *Astrophys. J.* **201**, 1 (1975).
- [31] P. Ivanov, P. Naselsky, and I. Novikov, *Phys. Rev. D* **50**, 7173 (1994).
- [32] J. Garcia-Bellido, A. D. Linde, and D. Wands, *Phys. Rev. D* **54**, 6040 (1996), [arXiv:astro-ph/9605094](#).
- [33] P. Ivanov, *Phys. Rev. D* **57**, 7145 (1998), [arXiv:astro-ph/9708224](#).
- [34] S. Blinnikov, A. Dolgov, N. K. Porayko, and K. Postnov, *JCAP* **1611**, 036 (2016), [arXiv:1611.00541 \[astro-ph.HE\]](#).
- [35] T. Nakamura, M. Sasaki, T. Tanaka, and K. S. Thorne, *Astrophys. J. Lett.* **487**, L139 (1997), [arXiv:astro-ph/9708060](#).
- [36] K. Ioka, T. Chiba, T. Tanaka, and T. Nakamura, *Phys. Rev. D* **58**, 063003 (1998), [arXiv:astro-ph/9807018](#).
- [37] M. Sasaki, T. Suyama, T. Tanaka, and S. Yokoyama, *Class. Quant. Grav.* **35**, 063001 (2018), [arXiv:1801.05235 \[astro-ph.CO\]](#).
- [38] A. M. Green and B. J. Kavanagh, (2020), [arXiv:2007.10722 \[astro-ph.CO\]](#).
- [39] B. Carr, K. Kohri, Y. Sendouda, and J. Yokoyama, (2020), [arXiv:2002.12778 \[astro-ph.CO\]](#).
- [40] S. Bird, I. Cholis, J. B. Muñoz, Y. Ali-Haïmoud, M. Kamionkowski, E. D. Kovetz, A. Raccanelli, and A. G. Riess, *Phys. Rev. Lett.* **116**, 201301 (2016), [arXiv:1603.00464 \[astro-ph.CO\]](#).
- [41] S. Clesse and J. García-Bellido, *Phys. Dark Univ.* **15**, 142 (2017), [arXiv:1603.05234 \[astro-ph.CO\]](#).
- [42] M. Sasaki, T. Suyama, T. Tanaka, and S. Yokoyama, *Phys. Rev. Lett.* **117**, 061101 (2016), [erratum: *Phys. Rev. Lett.* **121**, no.5, 059901 (2018)], [arXiv:1603.08338 \[astro-ph.CO\]](#).
- [43] Y. N. Eroshenko, *J. Phys. Conf. Ser.* **1051**, 012010 (2018), [arXiv:1604.04932 \[astro-ph.CO\]](#).
- [44] S. Wang, Y.-F. Wang, Q.-G. Huang, and T. G. F. Li, *Phys. Rev. Lett.* **120**, 191102 (2018), [arXiv:1610.08725 \[astro-ph.CO\]](#).
- [45] Y. Ali-Haïmoud, E. D. Kovetz, and M. Kamionkowski, *Phys. Rev. D* **96**, 123523 (2017), [arXiv:1709.06576 \[astro-ph.CO\]](#).
- [46] M. Raidal, C. Spethmann, V. Vaskonen, and H. Veermäe, *JCAP* **02**, 018 (2019), [arXiv:1812.01930 \[astro-ph.CO\]](#).
- [47] G. Hütsi, M. Raidal, and H. Veermäe, *Phys. Rev. D* **100**, 083016 (2019), [arXiv:1907.06533 \[astro-ph.CO\]](#).
- [48] V. Vaskonen and H. Veermäe, *Phys. Rev. D* **101**, 043015 (2020), [arXiv:1908.09752 \[astro-ph.CO\]](#).
- [49] A. D. Gow, C. T. Byrnes, A. Hall, and J. A. Peacock, *JCAP* **01**, 031 (2020), [arXiv:1911.12685 \[astro-ph.CO\]](#).
- [50] Y. Wu, *Phys. Rev. D* **101**, 083008 (2020), [arXiv:2001.03833 \[astro-ph.CO\]](#).
- [51] V. De Luca, G. Franciolini, P. Pani, and A. Riotto, *JCAP* **04**, 052 (2020), [arXiv:2003.02778 \[astro-ph.CO\]](#).
- [52] A. Hall, A. D. Gow, and C. T. Byrnes, (2020), [arXiv:2008.13704 \[astro-ph.CO\]](#).
- [53] V. De Luca, V. Desjacques, G. Franciolini, and A. Riotto, (2020), [arXiv:2009.04731 \[astro-ph.CO\]](#).
- [54] K. W. K. Wong, G. Franciolini, V. De Luca, V. Baibhav, E. Berti, P. Pani, and A. Riotto, *Phys. Rev. D* **103**, 023026 (2021), [arXiv:2011.01865 \[gr-qc\]](#).
- [55] G. Hütsi, M. Raidal, V. Vaskonen, and H. Veermäe, *JCAP* **2103**, 068 (2021), [arXiv:2012.02786 \[astro-ph.CO\]](#).
- [56] V. De Luca, G. Franciolini, P. Pani, and A. Riotto, (2021), [arXiv:2102.03809 \[astro-ph.CO\]](#).
- [57] M. Zevin, S. S. Bavera, C. P. L. Berry, V. Kalogera, T. Fragos, P. Marchant, C. L. Rodriguez, F. Antonini, D. E. Holz, and C. Pankow, *Astrophys. J.* **910**, 152 (2021), [arXiv:2011.10057 \[astro-ph.HE\]](#).
- [58] M. Zevin, C. Pankow, C. L. Rodriguez, L. Sampson, E. Chase, V. Kalogera, and F. A. Rasio, *Astrophys. J.* **846**, 82 (2017), [arXiv:1704.07379 \[astro-ph.HE\]](#).
- [59] Y. Bouffanais, M. Mapelli, D. Gerosa, U. N. Di Carlo, N. Giacobbo, E. Berti, and V. Baibhav, *Astrophys. J.* **886** (2019), 10.3847/1538-4357/ab4a79, [arXiv:1905.11054 \[astro-ph.HE\]](#).
- [60] K. W. K. Wong, K. Breivik, K. Kremer, and T. Callister, (2020), [arXiv:2011.03564 \[astro-ph.HE\]](#).
- [61] C. Kimball *et al.*, (2020), [arXiv:2011.05332 \[astro-ph.HE\]](#).
- [62] V. De Luca, G. Franciolini, P. Pani, and A. Riotto, *JCAP* **06**, 044 (2020), [arXiv:2005.05641 \[astro-ph.CO\]](#).
- [63] T. Fragos *et al.*, (2021), in preparation.
- [64] K. Breivik *et al.*, (2019), [arXiv:1911.00903 \[astro-ph.HE\]](#).
- [65] B. Paxton, R. Smolec, J. Schwab, A. Gaulty, L. Bildsten, M. Cantiello, A. Dotter, R. Farmer, J. A. Goldberg, A. S. Jermyn, S. M. Kanbur, P. Marchant, A. Thoul, R. H. D. Townsend, W. M. Wolf, M. Zhang, and F. X. Timmes, *ApJS* **243**, 10 (2019), [arXiv:1903.01426 \[astro-ph.SR\]](#).
- [66] F. Antonini, M. Gieles, and A. Gualandris, *Mon. Not. Roy. Astron. Soc.* **486**, 5008 (2019), [arXiv:1811.03640 \[astro-ph.HE\]](#).
- [67] M. Mirbabayi, A. Gruzinov, and J. Noreña, *JCAP* **2003**, 017 (2020), [arXiv:1901.05963 \[astro-ph.CO\]](#).
- [68] V. De Luca, V. Desjacques, G. Franciolini, A. Malhotra, and A. Riotto, *JCAP* **1905**, 018 (2019), [arXiv:1903.01179 \[astro-ph.CO\]](#).
- [69] S. Vitale, D. Gerosa, W. M. Farr, and S. R. Taylor, (2020), [arXiv:2007.05579 \[astro-ph.IM\]](#).
- [70] D. Foreman-Mackey, D. W. Hogg, D. Lang, and J. Goodman, *PASP* **125**, 306 (2013), [arXiv:1202.3665 \[astro-ph.IM\]](#).

- [71] C. Pankow, L. Sampson, L. Perri, E. Chase, S. Coughlin, M. Zevin, and V. Kalogera, *Astrophys. J.* **834**, 154 (2017), [arXiv:1610.05633 \[astro-ph.HE\]](#).
- [72] S. Vitale, D. Gerosa, C.-J. Haster, K. Chatziioannou, and A. Zimmerman, *Phys. Rev. Lett.* **119**, 251103 (2017), [arXiv:1707.04637 \[gr-qc\]](#).
- [73] M. Zevin, C. P. L. Berry, S. Coughlin, K. Chatziioannou, and S. Vitale, *Astrophys. J. Lett.* **899**, L17 (2020), [arXiv:2006.11293 \[astro-ph.HE\]](#).
- [74] S. Bhagwat, V. De Luca, G. Franciolini, P. Pani, and A. Riotto, *JCAP* **01**, 037 (2021), [arXiv:2008.12320 \[astro-ph.CO\]](#).
- [75] H. Jeffreys, *The Theory of Probability (3rd ed.)*, Oxford, England (1998).
- [76] R. Abbott *et al.* (LIGO Scientific, Virgo), *Astrophys. J. Lett.* **896**, L44 (2020), [arXiv:2006.12611 \[astro-ph.HE\]](#).
- [77] N. Fernandez and S. Profumo, *JCAP* **08**, 022 (2019), [arXiv:1905.13019 \[astro-ph.HE\]](#).
- [78] J. García-Bellido, J. F. Nuño Siles, and E. Ruiz Morales, *Phys. Dark Univ.* **31**, 100791 (2021), [arXiv:2010.13811 \[astro-ph.CO\]](#).
- [79] S. Hild *et al.*, *Class. Quant. Grav.* **28**, 094013 (2011), [arXiv:1012.0908 \[gr-qc\]](#).
- [80] S. Dwyer, D. Sigg, S. W. Ballmer, L. Barsotti, N. Mavalala, and M. Evans, *Phys. Rev. D* **91**, 082001 (2015), [arXiv:1410.0612 \[astro-ph.IM\]](#).
- [81] M. Maggiore *et al.*, *JCAP* **03**, 050 (2020), [arXiv:1912.02622 \[astro-ph.CO\]](#).
- [82] S. Vitale and M. Evans, *Phys. Rev. D* **95**, 064052 (2017), [arXiv:1610.06917 \[gr-qc\]](#).
- [83] K. K. Y. Ng, S. Vitale, W. M. Farr, and C. L. Rodriguez, (2020), [arXiv:2012.09876 \[astro-ph.CO\]](#).
- [84] R. Schneider, A. Ferrara, B. Ciardi, V. Ferrari, and S. Matarrese, *Mon. Not. Roy. Astron. Soc.* **317**, 385 (2000), [arXiv:astro-ph/9909419](#).
- [85] R. Schneider, A. Ferrara, P. Natarajan, and K. Omukai, *Astrophys. J.* **571**, 30 (2002), [arXiv:astro-ph/0111341](#).
- [86] R. Schneider, A. Ferrara, R. Salvaterra, K. Omukai, and V. Bromm, *Nature* **422**, 869 (2003), [arXiv:astro-ph/0304254](#).
- [87] T. Hartwig, M. Volonteri, V. Bromm, R. S. Klessen, E. Barausse, M. Magg, and A. Stacy, *Mon. Not. Roy. Astron. Soc.* **460**, L74 (2016), [arXiv:1603.05655 \[astro-ph.GA\]](#).
- [88] K. Belczynski, T. Ryu, R. Perna, E. Berti, T. L. Tanaka, and T. Bulik, *Mon. Not. Roy. Astron. Soc.* **471**, 4702 (2017), [arXiv:1612.01524 \[astro-ph.HE\]](#).
- [89] S. Vitale, W. M. Farr, K. Ng, and C. L. Rodriguez, *Astrophys. J. Lett.* **886**, L1 (2019), [arXiv:1808.00901 \[astro-ph.HE\]](#).
- [90] B. Liu and V. Bromm, *Mon. Not. Roy. Astron. Soc.* **495**, 2475 (2020), [arXiv:2003.00065 \[astro-ph.CO\]](#).
- [91] R. Valiante, M. Colpi, R. Schneider, A. Mangiagli, M. Bonetti, G. Cerini, S. Fairhurst, F. Haardt, C. Mills, and A. Sesana, *Mon. Not. Roy. Astron. Soc.* **500**, 4095 (2020), [arXiv:2010.15096 \[astro-ph.GA\]](#).
- [92] S. M. Koushiappas and A. Loeb, *Phys. Rev. Lett.* **119**, 221104 (2017), [arXiv:1708.07380 \[astro-ph.CO\]](#).
- [93] V. Baibhav, E. Berti, V. De Luca, G. Franciolini, K. K. Ng, P. Pani, A. Riotto, S. Vitale, and K. W. K. Wong, in preparation.
- [94] M. Zevin, “<https://doi.org/10.5281/zenodo.4448170>,” (2021).
- [95] M. Dominik, E. Berti, R. O’Shaughnessy, I. Mandel, K. Belczynski, C. Fryer, D. E. Holz, T. Bulik, and F. Pannarale, *Astrophys. J.* **806**, 263 (2015), [arXiv:1405.7016 \[astro-ph.HE\]](#).
- [96] L. S. Finn and D. F. Chernoff, *Phys. Rev. D* **47**, 2198 (1993), [arXiv:gr-qc/9301003 \[gr-qc\]](#).
- [97] L. S. Finn, *Phys. Rev. D* **53**, 2878 (1996), [arXiv:gr-qc/9601048](#).
- [98] B. P. Abbott *et al.* (LIGO Scientific, Virgo), *Astrophys. J. Lett.* **833**, L1 (2016), [arXiv:1602.03842 \[astro-ph.HE\]](#).
- [99] B. P. Abbott *et al.* (LIGO Scientific, Virgo), *Astrophys. J.* **882**, L24 (2019), [arXiv:1811.12940 \[astro-ph.HE\]](#).
- [100] B. P. Abbott *et al.* (KAGRA, LIGO Scientific, VIRGO), *Living Rev. Rel.* **21**, 3 (2018), [arXiv:1304.0670 \[gr-qc\]](#).
- [101] A. Nitz, I. Harry, D. Brown, C. M. Biwer, J. Willis, T. D. Canton, C. Capano, L. Pekowsky, T. Dent, A. R. Williamson, G. S. Davies, S. De, M. Cabero, B. Machenschalk, P. Kumar, S. Reyes, D. Macleod, dfinstad, F. Pannarale, T. Massinger, S. Kumar, M. Tápai, L. Singer, S. Khan, S. Fairhurst, A. Nielsen, S. Singh, shasvath, and B. U. V. Gadre, “[gwastro/pycbc: 1.18.0 release of pycbc](#),” (2021).
- [102] “<https://dcc.ligo.org/ligo-p1800370/public>,” (2018).
- [103] “<https://dcc.ligo.org/ligo-p2000223/public>,” (2020).